

Height Prediction and Refinement from Aerial Images with Semantic and Geometric Guidance

Mahdi Elhousni
Worcester Polytechnic Institute
melhousni@wpi.edu

Ziming Zhang
Worcester Polytechnic Institute
zzhang15@wpi.edu

Xinming Huang
Worcester Polytechnic Institute
xhuang@wpi.edu

Abstract—Deep learning provides a powerful new approach to many computer vision tasks. Height prediction from aerial images is one of those tasks that benefited greatly from the deployment of deep learning which replaced old multi-view geometry techniques. This letter proposes a two-stage approach, where first a multi-task neural network is used to predict the height map resulting from a single RGB aerial input image. We also include a second refinement step, where a denoising autoencoder is used to produce higher quality height maps. Experiments on two publicly available datasets show that our method is capable of producing state-of-the-art results. Code is publicly available¹.

I. INTRODUCTION

Lately, the abundance of aerial imagery has made the use of deep learning much more prevalent in UAV related challenges. Height prediction, semantic segmentation and object detection are some of the most popular tasks in this area and are routinely featured in numerous challenges offered each year.

We focus on the height prediction task, where based on an input RGB aerial image, we are supposed to predict and reconstruct the corresponding height map, or in other words, predict the height value of each pixel in the input image. Predicting such height maps can be very useful in subsequent UAV related challenges such as building and roof reconstruction or 3D mesh production. This is traditionally done using Structure from Motion (SfM) techniques and stereo camera rigs, however, more methods revolving around deep learning networks have been presented in the literature lately and show great potential.

We explore this challenge through a multi-task learning framework where additional results are produced and used to improve the main height prediction results. Previous works have already proposed and showed that multi-task learning helps improving the accuracy of height prediction networks by including semantic labels. We propose to add a third branch in our multi-task network which will be devoted to predicting the surface normals, as shown on Figure 1. In this configuration, the main height prediction branch will have access to both semantic and geometric guidance, helping it to predict height values more accurately.

However, since our only input is a single RGB image, our predictions are bound to be noisy due to artefacts such as shadows or unexpected changes in color. Therefore, we also

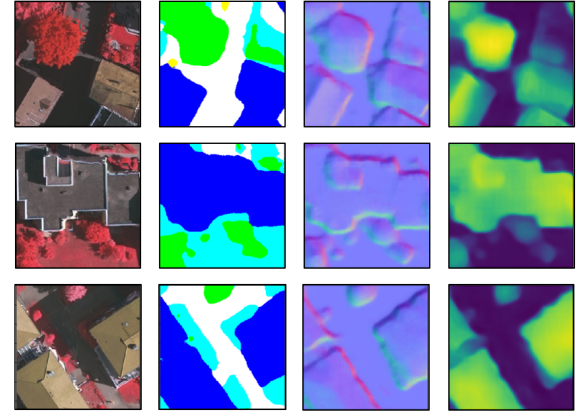


Fig. 1. The outputs of our multi-task network. From left to right: The input RGB image, the output semantic labels, surface normals and height predictions.

propose to introduce a refinement step where a denoising autoencoder is leveraged and fed all the outputs of the prediction step in order to produce higher quality and more accurate height maps.

Specifically, our contributions in this letter are:

- We propose a triple-branch network, based on pretrained off-the-shelf encoders, for semantic labels, surface normals and height prediction.
- We introduce a denoising autoencoder as a refinement step for our final height maps.
- We achieve state-of-the-art performance on two publicly available datasets, and an extensive ablation study shows the importance of each step in our reconstruction pipeline.

II. RELATED WORK

Height prediction from aerial images: This task has been receiving increasing attention by the deep learning and remote sensing communities, especially after the use of UAVs to collect aerial data has become widespread and accessible. In works such as [1], [9], [16], deep learning methods such as residual networks, skip connections and generative adversarial networks are leveraged in order to predict height maps using only an RGB aerial image as input. Other works such as [3], [19], proposed to reformulate the task as a multi-learning problem, by introducing neural networks capable of predicting both

¹<https://github.com/melhousni/DSMNet>

the height maps and the semantic labels simultaneously. These works showed that both outputs benefit from the presence of the other, during the simultaneous optimization process of the multi-task network. We chose to extend that formulation by including a third branch in our network, tasked with predicting surface normals, which was inspired by previous works [6], [7] in the depth prediction task for autonomous driving cars. Surface normals are also known to be extremely useful during 3D reconstruction tasks and is required for surface reconstruction algorithms such as the Poisson surface reconstruction algorithm [13] or the Ball pivoting algorithm [2].

Denoising Autoencoders: Autoencoders are a popular neural network architecture that has shown to be powerful across multiple tasks such as segmentation of medical imagery [17], decoding the semantic meaning of words [15] or solving facial recognition challenges [11]. One of the most useful type of autoencoders available in the literature is the denoising autoencoder: [20] has shown that autoencoders can be trained and used to remove noise from an arbitrary input signal such as an image. We propose to use denoising autoencoder to refine the height prediction of our multi-task learning network.

III. METHOD

A. Problem setup

Our main objective here is to predict an accurate height map using only a monocular aerial image as input. Fundamentally, we are trying to solve a non-linear regression problem which can be formulated as:

$$\min_{\psi \in \Psi} \sum_i \ell(\mathbf{y}_i, \psi(\mathbf{x}_i)) \quad (1)$$

where $\psi : \mathcal{X} \rightarrow \mathcal{Y}$ denotes the height prediction mapping function from the feasible space Ψ , $\ell : \mathcal{Y} \times \mathcal{Y} \rightarrow \mathbb{R}$ denotes a loss function such as the least-square, \mathbf{x}_i is the input aerial image and \mathbf{y}_i is the output height map.

Predicting height only using a single aerial image is possible. However, previous works such as [3], [19] showed that including additional branches to predict other related information such as segmentation labels can be beneficial for both tasks. In our case, in addition to predicting the height maps, we also predict semantic labels and surface normals, which provide semantic and geometric guidance by augmenting the main height branch with information from the semantics and normals branches. More details on this can be found in the height prediction section below. Keeping that in mind, our ψ function can now be defined as:

$$\psi(\mathbf{x}_i) = \{\mathbf{P}_h, \mathbf{P}_s, \mathbf{P}_n\} \quad (2)$$

where \mathbf{P}_h , \mathbf{P}_s and \mathbf{P}_n are the height, semantic and surface normal predictions respectively, that are trying to approximate $\mathbf{y}_i = \{\mathbf{P}_h^*, \mathbf{P}_s^*, \mathbf{P}_n^*\}$ where \mathbf{P}_h^* , \mathbf{P}_s^* and \mathbf{P}_n^* are the height, semantic and surface normal ground truth respectively. Finding a good approximation of the ψ function can be seen as the first stage in our proposed method.

Regression problems such as the one we are facing are difficult to solve: Attempting to predict the exact height value of each pixel in a (20000x20000) tile is near impossible, and only an approximation of the ground truth can be achieved. This makes our height prediction \mathbf{P}_h noisy by definition, so the use of denoising autoencoders is appropriate in this situation.

First, we can write: $\mathbf{P}_h = \mathbf{P}'_h + e$ where \mathbf{P}'_h is the clean height value, and e the noise inherent to our approximation of the function ψ . By introducing a denoising autoencoder, we can approximate the noise function γ such as $\mathbf{P}_h = \mathbf{P}'_h + \gamma(\mathbf{z}_i)$, where \mathbf{z}_i is the concatenation of the outputs of ψ with the input aerial image x_i . This makes it possible to re-write equations (2) as $\psi(\mathbf{x}_i) = \{\mathbf{P}'_h + \gamma(\mathbf{z}_i), \mathbf{P}_s, \mathbf{P}_n\}$. We can also now define the objective of the second stage of our method such as:

$$\min_{\gamma \in \Gamma} \sum_i \ell(\mathbf{P}_h^*, \mathbf{P}_h - \gamma(\mathbf{z}_i)) \quad (3)$$

In this paper, our goal is to approximate both function ψ and γ by using two cascaded deep neural networks.

B. Height prediction

We solve the height prediction problem here via multi-task learning where, in addition to the main height prediction, semantic and surface normals predictions are conducted too. We found that by re-routing the information in the semantic and surface normal branches to the main height branch, our neural network can learn to predict better values, especially around edges.

Figure 2 shows our multi-task learning network architecture. We propose a neural network where we combine a pretrained encoder (tasked with extracting relevant features from the input aerial images), with three interconnected decoder branches for each of the three expected predictions. We choose to use a DenseNet121 network, pretrained on ImageNet, as our main encoder. We show later in the experimentation part that compared to other popular ar-

Fig. 2. Architecture of our multi-task learning network for height, semantic and surface normals predictions. Note that each tconv block is followed by the ReLu function and drop out layers are inserted after each tconv layers in the main height prediction branch.

chitectures, DenseNet121 yields the best accuracy. Our decoders on the other hand is inspired by [14] and are characterized by being able to reconstruct the expected predictions efficiently.

This network is optimized by using a multi-objective loss defined as:

where \mathbf{P}_h^* , \mathbf{P}_s^* and \mathbf{P}_n^* are the height, semantic and surface normal ground truth respectively. Finding a good approximation of the ψ function can be seen as the first stage in our proposed method.

the height maps and the semantic labels simultaneously. These works showed that both outputs benefit from the presence of the other, during the simultaneous optimization process of the multi-task network. We chose to extend that formulation by including a third branch in our network, tasked with predicting surface normals, which was inspired by previous works [6], [7] in the depth prediction task for autonomous driving cars. Surface normals are also known to be extremely useful during 3D reconstruction tasks and is required for surface reconstruction algorithms such as the Poisson surface reconstruction algorithm [13] or the Ball pivoting algorithm [2].

Denoising Autoencoders: Autoencoders are a popular neural network architecture that has shown to be powerful across multiple tasks such as segmentation of medical imagery [17], decoding the semantic meaning of words [15] or solving facial recognition challenges [11]. One of the most useful type of autoencoders available in the literature is the denoising autoencoder: [20] has shown that autoencoders can be trained and used to remove noise from an arbitrary input signal such as an image. We propose to use denoising autoencoder to refine the height prediction of our multi-task learning network.

III. METHOD

A. Problem setup

Our main objective here is to predict an accurate height map using only a monocular aerial image as input. Fundamentally, we are trying to solve a non-linear regression problem which can be formulated as:

$$\min_{\psi \in \Psi} \sum_i \ell(\mathbf{y}_i, \psi(\mathbf{x}_i)) \quad (1)$$

where $\psi : \mathcal{X} \rightarrow \mathcal{Y}$ denotes the height prediction mapping function from the feasible space Ψ , $\ell : \mathcal{Y} \times \mathcal{Y} \rightarrow \mathbb{R}$ denotes a loss function such as the least-square, \mathbf{x}_i is the input aerial image and \mathbf{y}_i is the output height map.

Predicting height only using a single aerial image is possible. However, previous works such as [3], [19] showed that including additional branches to predict other related information such as segmentation labels can be beneficial for both tasks. In our case, in addition to predicting the height maps, we also predict semantic labels and surface normals, which provide semantic and geometric guidance by augmenting the main height branch with information from the semantics and normals branches. More details on this can be found in the height prediction section below. Keeping that in mind, our ψ function can now be defined as:

$$\psi(\mathbf{x}_i) = \{\mathbf{P}_h, \mathbf{P}_s, \mathbf{P}_n\} \quad (2)$$

where \mathbf{P}_h , \mathbf{P}_s and \mathbf{P}_n are the height, semantic and surface normal predictions respectively, that are trying to approximate $\mathbf{y}_i = \{\mathbf{P}_h^*, \mathbf{P}_s^*, \mathbf{P}_n^*\}$ where \mathbf{P}_h^* , \mathbf{P}_s^* and \mathbf{P}_n^* are the height, semantic and surface normal ground truth respectively. Finding a good approximation of the ψ function can be seen as the first stage in our proposed method.

the height maps and the semantic labels simultaneously. These works showed that both outputs benefit from the presence of the other, during the simultaneous optimization process of the multi-task network. We chose to extend that formulation by including a third branch in our network, tasked with predicting surface normals, which was inspired by previous works [6], [7] in the depth prediction task for autonomous driving cars. Surface normals are also known to be extremely useful during 3D reconstruction tasks and is required for surface reconstruction algorithms such as the Poisson surface reconstruction algorithm [13] or the Ball pivoting algorithm [2].

Denoising Autoencoders: Autoencoders are a popular neural network architecture that has shown to be powerful across multiple tasks such as segmentation of medical imagery [17], decoding the semantic meaning of words [15] or solving facial recognition challenges [11]. One of the most useful type of autoencoders available in the literature is the denoising autoencoder: [20] has shown that autoencoders can be trained and used to remove noise from an arbitrary input signal such as an image. We propose to use denoising autoencoder to refine the height prediction of our multi-task learning network.

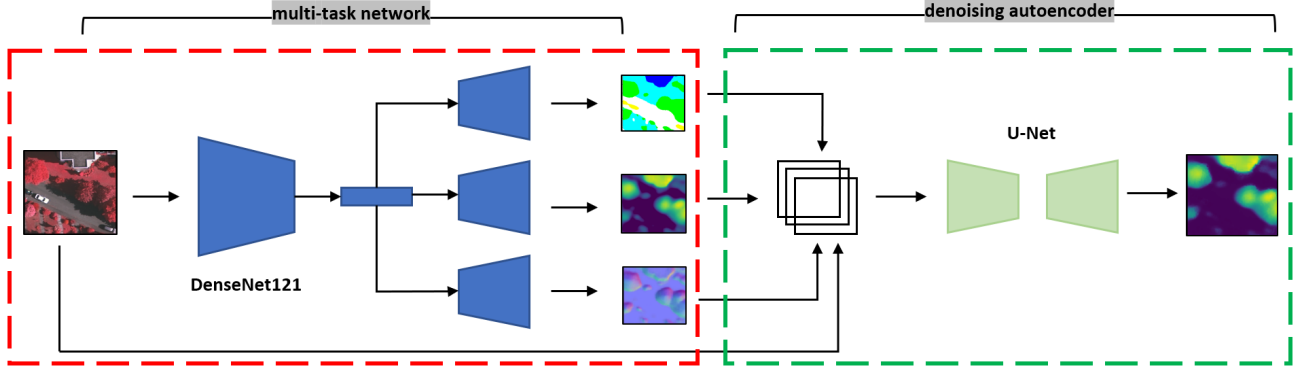


Fig. 3. Our two stage height prediction and refinement pipeline. We use DenseNet121 to extract a global feature vector from the input aerial images, which is used to predict the normals map, semantic labels and a first guess at the height map (first stage, in red). These results are concatenated with the input aerial image and fed into a denoising autoencoder to generate the refined final height map (second stage, in green).

$$\mathcal{L} = w_1 \mathcal{L}_h + w_2 \mathcal{L}_s + w_3 \mathcal{L}_n \quad (4)$$

where $\mathcal{L}_h = \frac{1}{n} \sum_{i=1}^n (P_h - P_h^*)^2$, $\mathcal{L}_s = -\frac{1}{n} \sum_{i=1}^n P_s^* \log(P_s)$, $\mathcal{L}_n = \frac{1}{n} \sum_{i=1}^n (P_n - P_n^*)^2$ and w_1, w_2 and w_3 are weights set up according to the training dataset and the scale of each loss function.

C. Height refinement

As mentioned before, our height prediction map P_h is noisy and can be considered an initial guess at the final height prediction P'_h . We introduce an autoencoder in order to estimate the said noise and produce higher quality height map predictions.

We choose the popular U-Net architecture [17] as network structure, and use as an input the concatenation of the outputs from the previous multi-task network P_h, P_s and P_n with the aerial image \mathbf{x}_i , as shown in Figure 3. The loss function used to optimize the refinement autoencoder is the mean square error between the refined height map and the ground truth : $\mathcal{L}_r = \frac{1}{n} \sum_{i=1}^n (P'_h - P_h^*)^2 = \frac{1}{n} \sum_{i=1}^n (P_h - \gamma - P_h^*)^2$.

IV. EXPERIMENTS

A. Datasets

2018 DFC [22] : This dataset was released during the 2018 Data Fusion Contest organized by the Image Analysis and Data Fusion Technical Committee of the IEEE Geoscience and Remote Sensing Society. It was collected over the city of Houston, and contains multiple optical resources geared toward urban machine learning tasks such multispectral LiDAR, hyperspectral imaging, Very High-Resolution (VHR) imagery and semantic labels. Using the results of the multispectral LiDAR, it is possible to generate Digital Structural Models (DSM) and Digital Elevation Models (DEM), which, if subtracted from one another, produces height maps that we can use as ground truth. 4 tiles are used for training while 10 are used for testing.

ISPRS Vaihingen [5] : This dataset was released during the semantic labeling contest of ISPRS WG III/4. It was collected

over the city of Vaihingen, Germany and consists of very high resolution true ortho photo (TOP) tiles and corresponding Digital Surface Models (DSM) and semantic labels. As it is usually done when dealing with this dataset, we use the normalized DSM (nDSM) produced by [8] as ground truth for our height prediction. 16 tiles were used for training while 17 tiles are used for testing.

Surface normal maps : The surface normal maps for both dataset are generated using the given height maps, following practices usually used for surface normals estimation from dense depth maps based on the Sobel operator. The details are listed in Alg 1.

Algorithm 1: Surface normals generation

```

Input : Height map  $P_h$ 
Output: Surface normals map  $P_n$ 
 $zx \leftarrow \text{Sobel}(P_h, 0)$ 
 $zy \leftarrow \text{Sobel}(P_h, 1)$ 
 $N \leftarrow \text{stack}(-zx, -zy, 1)$ 
 $P_n \leftarrow \frac{N/\|N\|}{2} + 1$ 
return  $P_n$ 

```

B. Height prediction and refinement

Training : Our training process has two stages: we first remove the denoising autoencoder and only focus on training the multi-task network. To do so, random 320x320 crops are sampled from the aerial tiles and corresponding semantic, surface normals and height ground truth, and are used for training. Once the multi-task network converges, we freeze its weights and plug in the denoising autoencoder to refine our height predictions. We train this second network following the same random sampling process used to train the first one. Note that in the case of the DFC2018 dataset, the input VHR aerial tiles are ten times bigger than their corresponding DSM, DEM and semantic labels. To deal with that, we first down sample the aerial tiles ten times before starting to collect training crops.

Results : The aerial tiles were reconstructed using a rolling window of the same size of the training samples and with a constant step size. We also use Gaussian smoothing to deal with overlapping areas. We report the results of our height prediction and refinement pipeline on both the datasets cited before in Table I. When comparing with previous proposed methods in the literature, we can see that by using our multi-task network combined with our refinement step, we are able to surpass the state-of-the-art scores across all metrics on both datasets, with sometimes improvement up to 25%.

It is especially interesting to note that we are able to achieve similar scores to methods which were trained on the VHR aerial tiles directly without any down sampling as shown in Table II. Such networks would need much longer time than our method to reconstruct the same size output height tiles.

TABLE I
COMPARISON WITH OTHER HEIGHT PREDICTION METHODS ON THE ISPRS VAIHINGEN AND THE 2018 DFC DATASETS.

Method	ISPRS Vaihingen			2018 DFC		
	MSE	MAE	RMSE	MSE	MAE	RMSE
Ours	0.0042	0.036	0.062	6.92	1.37	2.57
Carvalho [3]	0.0060	0.045	0.074	9.34	1.53	2.97
Srivastava [19]	-	0.063	0.098	-	-	-
IMG2DSM [9]	-	-	0.090	-	-	-

TABLE II
COMPARISON WITH METHOD TRAINED ON VHR AERIAL IMAGES.

Method	MSE	MAE	RMSE	Time (s)	Input Resolution
Ours	6.92	1.37	2.57	72	1192x1202
Carvalho VHR [3]	7.27	1.26	2.59	774	11920x12020

C. Semantic label and surface normal predictions

Even though we do not focus on the semantic label and surface normal predictions and only use them to improve the height predictions, we share the results of those two branches and compare them with available methods in the literature in Table III. Our results show that our multi-task network is able to produce semantic label results that are comparable with the state of the art on the Vaihingen dataset and acceptable ones on the DFC2018 (which has 20 classes compared to the 6 of the Vaihingen dataset). It is also able to produce meaningful surface normal maps as seen on Figure 1.

TABLE III
SEMANTIC LABELS AND SURFACE NORMALS RESULTS ON THE ISPRS VAIHINGEN AND THE 2018 DFC DATASETS.

Method	ISPRS Vaihingen			2018 DFC		
	Semantic Labels			Surface Normals		
Method	OA	AA	Kappa	OA	AA	Kappa
Ours	85.6	74.8	80.1	51.89	47.01	49
Carvalho [3]	87.7	85.4	75.9	64.70	58.85	63
Srivastava [19]	78.8	73.4	71.9	-	-	-
Cerra [4]	-	-	-	58.60	55.60	56
Fusion-FCN [21]	-	-	-	63.28	-	61
Method	MSE	MAE	RMSE	MSE	MAE	RMSE
Ours	0.0115	0.0642	0.1066	0.0620	0.2119	0.2572

D. Ablation study

Height refinement : To demonstrate the usefulness of our additional refinement step, we test our method with and without the denoising autoencoder, on both available datasets. In Table IV, we compare the results obtained after both experiments and show that the refinement step always produces more accurate height maps, bringing sometimes an increase of up to 16% in accuracy.

TABLE IV
COMPARISON OF OUR HEIGHT PREDICTION METHODS WITH AND WITHOUT REFINEMENT, ON THE ISPRS VAIHINGEN AND THE 2018 DFC DATASETS.

Method	ISPRS Vaihingen			2018 DFC		
	MSE	MAE	RMSE	MSE	MAE	RMSE
multi-task only	0.0045	0.043	0.065	7.36	1.50	2.64
multi-task + refinement	0.0042	0.036	0.062	6.92	1.37	2.57

We also show qualitatively on Figure 4 that the refinement height maps are much closer to the ground truth and contains less noise than the direct output of the multi-task network.

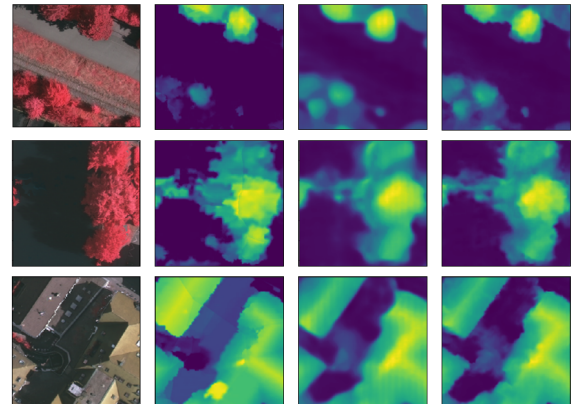


Fig. 4. Qualitative comparison. From left to right: The input RGB image, the height prediction of our multi-task network, the refined height map of our denoising autoencoder and the ground truth.

Choosing the right encoder : Our network structure for height prediction is flexible, since any off-the shelf encoder can be used in the first stage to extract features from the input aerial image.

TABLE V
ENCODER COMPARISON ON THE DFC2018 DATASET.

Encoder	MSE	MAE	RMSE
ResNet101 [10]	18.95	3.33	4.19
VGG19 [18]	8.57	1.87	2.85
DenseNet121 [12]	7.36	1.50	2.64

However, we show in Table V that DenseNet121 outperforms other popular encoder structures and produces the most accurate height maps. To ensure fairness, all the networks were trained for the same number of epochs and using the same hyper parameters, in order for us to be able to compare both the convergence speed and accuracy scores.

Geometric and semantic guidance : We show in this section, the effect of the geometric and semantic guidance on our method in both the prediction and refinement stages.

First, we show in Table VI that using a multi-task network instead of a single-task one, with three branches for height, semantic labels and surface normals, improves our overall height prediction results. We also show in Table VIII that by concatenating all the results of the first stage as the input to the denoising autoencoder, we are able to generate more accurate and refined results compared to only using the height image as input.

TABLE VI
COMPARISON OF HEIGHT PREDICTION RESULTS OF SINGLE AND
MULTI-TASK NETWORKS.

Method	ISPRS Vaihingen			2018 DFC		
	MSE	MAE	RMSE	MSE	MAE	RMSE
single-task	0.0048	0.046	0.067	8.17	1.64	2.78
multi-task	0.0045	0.043	0.065	7.36	1.50	2.64

TABLE VII
COMPARISON OF HEIGHT REFINEMENT RESULTS OF SINGLE AND
MULTI-INPUT DENOISER.

Method	ISPRS Vaihingen			2018 DFC		
	MSE	MAE	RMSE	MSE	MAE	RMSE
single-input	0.0043	0.037	0.063	7.13	1.47	2.62
multi-input	0.0042	0.036	0.062	6.92	1.37	2.57

Finding the right reconstruction step : The accuracy of our final tile reconstruction depends also on the step size of the rolling window that we use when collecting aerial crops. We show in Table VIII the different results corresponding to different step sizes. We found that a step size of 60 is the most optimal one across both datasets.

TABLE VIII
COMPARISON OF OUR RECONSTRUCTION RESULTS BASED ON THE STEP
SIZE.

Step	ISPRS Vaihingen			2018 DFC		
	MSE	MAE	RMSE	MSE	MAE	RMSE
80	0.00421	0.0363	0.0625	6.98	1.38	2.58
60	0.00420	0.0362	0.0623	6.92	1.37	2.57
40	0.00421	0.0362	0.0623	6.93	1.37	2.58

V. CONCLUSION

In this letter, we propose a two-stage pipeline to predict and refine height maps using an RGB aerial image only as input. We leverage the power of multi-task learning by designing a three-branch neural network for height, semantic labels and surface normals prediction. We also use a denoising autoencoder to refine our height maps and eliminate the noise inherent to the output of our first stage network and the ambiguities sometimes present in RGB images. Our experiments on two publicly available datasets and our comparison with proposed methods in the literature showed that our method is capable of producing state-of-the-art results in height prediction. In future work, we will explore how these predicted height maps could be used to improve other tasks such as 3D reconstruction or UAV localization.

REFERENCES

- [1] Hamed Amini Amirkolaei and Hossein Arefi. Height estimation from single aerial images using a deep convolutional encoder-decoder network. volume 149, pages 50–66. Elsevier, 2019.
- [2] Fausto Bernardini, Joshua Mittleman, Holly Rushmeier, Cláudio Silva, and Gabriel Taubin. The ball-pivoting algorithm for surface reconstruction. *IEEE transactions on visualization and computer graphics*, 5(4):349–359, 1999.
- [3] Marcela Carvalho, Bertrand Le Saux, Pauline Trouvé-Peloux, Frédéric Champagnat, and Andrés Almansa. Multitask learning of height and semantics from aerial images. IEEE, 2019.
- [4] Daniele Cerra et al. Combining deep and shallow neural networks with ad hoc detectors for the classification of complex multi-modal urban scenes. In *IGARSS 2018-2018 IEEE International Geoscience and Remote Sensing Symposium*, pages 3856–3859. IEEE, 2018.
- [5] Michael Cramer. The dgpf-test on digital airborne camera evaluation—overview and test design. *Photogrammetrie-Fernerkundung-Geoinformation*, 2010(2):73–82, 2010.
- [6] Thanuja Dharmasiri, Andrew Spek, and Tom Drummond. Joint prediction of depths, normals and surface curvature from rgb images using cnns. In *2017 IEEE/RSJ International Conference on Intelligent Robots and Systems (IROS)*, pages 1505–1512. IEEE, 2017.
- [7] David Eigen and Rob Fergus. Predicting depth, surface normals and semantic labels with a common multi-scale convolutional architecture. In *Proceedings of the IEEE international conference on computer vision*, pages 2650–2658, 2015.
- [8] Markus Gerke. Use of the stair vision library within the isprs 2d semantic labeling benchmark. 2014.
- [9] Pedram Ghamisi and Naoto Yokoya. Img2dsm: Height simulation from single imagery using conditional generative adversarial net. volume 15, pages 794–798. IEEE, 2018.
- [10] Kaiming He, Xiangyu Zhang, Shaoqing Ren, and Jian Sun. Deep residual learning for image recognition. In *Proceedings of the IEEE conference on computer vision and pattern recognition*, pages 770–778, 2016.
- [11] Geoffrey E Hinton, Alex Krizhevsky, and Sida D Wang. Transforming auto-encoders. In *International conference on artificial neural networks*, pages 44–51. Springer, 2011.
- [12] Gao Huang, Zhuang Liu, Laurens Van Der Maaten, and Kilian Q Weinberger. Densely connected convolutional networks. In *Proceedings of the IEEE conference on computer vision and pattern recognition*, pages 4700–4708, 2017.
- [13] Michael Kazhdan, Matthew Bolitho, and Hugues Hoppe. Poisson surface reconstruction.
- [14] Iro Laina, Christian Rupprecht, Vasileios Belagiannis, Federico Tombari, and Nassir Navab. Deeper depth prediction with fully convolutional residual networks. In *2016 Fourth international conference on 3D vision (3DV)*, pages 239–248. IEEE, 2016.
- [15] Cheng-Yuan Liou, Wei-Chen Cheng, Jiun-Wei Liou, and Daw-Ran Liou. Autoencoder for words. volume 139, pages 84–96. Elsevier, 2014.
- [16] C.-J. Liu et al. Im2elevation: Building height estimation from single-view aerial imagery. *MDPI Remote Sensing*, 2020.
- [17] Olaf Ronneberger, Philipp Fischer, and Thomas Brox. U-net: Convolutional networks for biomedical image segmentation. In *International Conference on Medical image computing and computer-assisted intervention*, pages 234–241. Springer, 2015.
- [18] Karen Simonyan and Andrew Zisserman. Very deep convolutional networks for large-scale image recognition. *arXiv preprint arXiv:1409.1556*, 2014.
- [19] Shivangi Srivastava, Michele Volpi, and Devis Tuia. Joint height estimation and semantic labeling of monocular aerial images with cnns. In *2017 IEEE International Geoscience and Remote Sensing Symposium (IGARSS)*, pages 5173–5176. IEEE, 2017.
- [20] Pascal Vincent et al. Stacked denoising autoencoders: Learning useful representations in a deep network with a local denoising criterion. volume 11, 2010.
- [21] Yonghao Xu, Bo Du, and Liangpei Zhang. Multi-source remote sensing data classification via fully convolutional networks and post-classification processing. In *IGARSS 2018-2018 IEEE International Geoscience and Remote Sensing Symposium*, pages 3852–3855. IEEE, 2018.
- [22] Yonghao Xu et al. Advanced multi-sensor optical remote sensing for urban land use and land cover classification: Outcome of the 2018 ieee grss data fusion contest. *IEEE Journal of Selected Topics in Applied Earth Observations and Remote Sensing*, 12(6):1709–1724, 2019.